

Synthesis of Hexagonal Boron Nitride Monolayer: Control of Nucleation and Crystal Morphology

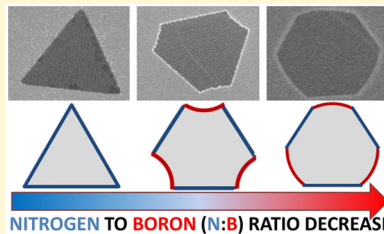
Yijing Stehle,[†] Harry M. Meyer III,[†] Raymond R. Unocic,[†] Michelle Kidder,[†] Georgios Polizos,[†] Panos G. Datskos,[†] Roderick Jackson,[‡] Sergei N. Smirnov,^{*,§} and Ivan V. Vlassiouk^{*,†}

[†]Oak Ridge National Laboratory, Oak Ridge, Tennessee 37831, United States

[‡]Department of Chemistry and Biochemistry, New Mexico State University, Las Cruces, New Mexico 88003, United States

Supporting Information

ABSTRACT: Monolayer hexagonal boron nitride (hBN) attracts significant attention due to the potential to be used as a complementary two-dimensional dielectric in fabrication of functional 2D heterostructures. Here we investigate the growth stages of the hBN single crystals and show that hBN crystals change their shape from triangular to truncated triangular and further to hexagonal depending on copper substrate distance from the precursor. We suggest that the observed hBN crystal shape variation is affected by the ratio of boron to nitrogen active species concentrations on the copper surface inside the CVD reactor. Strong temperature dependence reveals the activation energies for the hBN nucleation process of ~ 5 eV and crystal growth of ~ 3.5 eV. We also show that the resulting h-BN film morphology is strongly affected by the heating method of borazane precursor and the buffer gas. Elucidation of these details facilitated synthesis of high quality large area monolayer hexagonal boron nitride by atmospheric pressure chemical vapor deposition on copper using borazane as a precursor.



Atomically thin hexagonal boron nitride (hBN), also called “white graphene”, is an insulator (band gap ~ 6 eV) with a planar hexagonal lattice structure, quite similar to that of graphene, with only 1.7% lattice mismatch.^{1–5} Because of the strong covalent sp^2 bonds in the BN plane, hBN has high mechanical strength and good thermal conductivity, as well as excellent chemical and thermal stability.⁶ These properties make atomically thin hBN a great complementing material for graphene in creating a new class of functional multilayer heterostructures and devices.^{7–12} Hexagonal boron nitride has been previously reported to be a desirable dielectric substrate for high-performance graphene devices.^{7,8} Because of its atomically smooth surface, h-BN is free of dangling bonds and surface trapped charges. The electron mobility values of graphene film measured on an h-BN substrate are an order of magnitude higher than those for devices fabricated on SiO_2/Si substrates.^{7,8} Moreover, both experimental and theoretical studies reveal that graphene/h-BN/graphene stacks can be excellent thin film capacitors.^{9–11}

Similar to graphene, controlled synthesis of large-area high-quality hBN is important for both fundamental studies and commercial applications.¹³ Among the synthetic methods, chemical vapor deposition (CVD) has shown a great potential to prepare large-area hBN films, which opened up possibilities for the applications requiring large scale continuous hBN films.^{14,15} Compared to the low pressure CVD approach (LPCVD), atmospheric pressure CVD (APCVD) holds the benefit of a lower cost and better safety, but first reports expressed concern about APCVD being “uncontrollable” for the monolayer h-BN synthesis.^{13–16} In this report, we present a thorough analysis for APCVD growth process of h-BN on

copper substrate using borazane as a precursor that lead to controllable synthesis of large scale (2 in. \times 2 in.) monolayer h-BN films with large ($20\ \mu m$) single crystals.

EXPERIMENTAL SECTION

Growth. Samples were synthesized in a three zone furnace with 24 in. heating length using a 3 in. diameter quartz tube. Prior to the growth, copper foils (125 μm thick, Nimrod Hall) were cleaned in acetone and electropolished in a 1:3 mixture of poly(ethylene glycol)/phosphoric acid to reduce the surface roughness and remove contaminations.¹⁷ Electropolishing was found to be necessary for consistent hBN growth outcome not affected by copper surface contaminations such as carbonized oil residues and inorganic impurities. Electropolished copper substrates were placed in a furnace equipped with three thermocouples that were labeled as A, B, and C in the Figure 1a; the distance between them was 8 in. Foils were annealed at 1065 °C for 0.5 h in a 500 sccm flow of 2.5% H_2 in Ar.¹⁷ Most of the growth was done using 500 sccm of 2.5% H_2/Ar as a carrier gas except for growth in nitrogen atmosphere where 350 sccm of 2.5% H_2/N_2 was used instead (Figure 1c). All gases were ultrahigh purity grade (<1 ppm of O_2) and were used without additional purification. Borazane (Aldrich #682098) was used as the precursor for hBN growth. It was chosen because of the desired B to N ratio and its relatively low evaporation temperature. Typically, 2–3 mg of borazane was loaded into a specially designed half-opened boat made of nickel foil which can be moved by a magnet to a desired location in the upstream of CVD tube. The precursor temperature was controlled either by the distance to the CVD furnace or by a heating belt around the quartz tube at the precursor location. In the former case, the precursor

Received: September 14, 2015

Revised: November 9, 2015

Published: November 10, 2015

temperature was kept constant by moving the boat to the CVD tube region with temperature $T_{ev} = 85 \pm 5$ °C. After hBN deposition, the sample was quickly cooled down by turning off and opening the furnace while maintaining the same gas flow as during the deposition. To analyze the growth rate and morphology of individual single crystal domains, deposition was stopped after 30 min of growth (Figures 1, 3, and 4). Full coverage of the copper by hBN was achieved by longer deposition times (60 min at 1065 °C) and/or larger precursor mass of 7 mg with its controllable heating by heating belt, when necessary.

Characterization. The hBN crystal shape and size were analyzed using a scanning electron microscope, SEM (Zeiss, Merlin). hBN crystals were also visualized by oxidizing copper foils on a hot plate at 200 °C for 1 min (Figure 5a,b). Raman spectra were obtained using a Renishaw instrument with 633 nm laser excitation on hBN samples transferred on the SiO₂/Si wafer. The UV-vis spectrum of hBN transferred onto quartz was measured using a Varian Cary 5000 spectrophotometer. Atomic resolution imaging was obtained using Nion UltraSTEM operated at 60 kV, which is below the knock-on radiation damage of BN. Auger spectra and elemental maps were obtained using a Phi-680 Scanning Auger Nanoprobe. To transfer hBN onto the substrate of interest, first, hBN grown on copper foils was spin-coated with Microchem 49SPMMA A4 (2000 rpm), and, subsequently copper was etched away by 1 M FeCl₃ in 3% HCl solution. Resulting PMMA/hBN sandwich was washed in DI water several times and transferred on the substrate of interest. After drying overnight, PMMA was dissolved in acetone. Thermogravimetric analysis (TGA) was performed on a TA Instruments Q5000 at 5 °C/min rate using Ar as inert atmosphere.

RESULTS AND DISCUSSION

Growth of Separate Domains. In the CVD synthesis of 2D material such as graphene and hexagonal boron nitride, many parameters influence the growth process and the resulting quality of synthesized film. In CVD growth of hBN, the obvious parameters are the copper foil surface pretreatment, the growth temperature and atmosphere, the deposition time, and precursor dosage, and additional parameters arising from the nongaseous form of precursor that carries the two elements, B and N, have to be carefully controlled as well.

Domain Shape. Graphene crystals can take variety of shapes.¹⁸ Unlike graphene, hBN contains two different elements and thus have greater variation in crystal's termination groups. Generally, nitrogen termination is considered to be energetically favorable compared to the boron termination.⁵ Thus, most reports discussing hBN synthesis by CVD assign termination to nitrogen atoms in the typically observed triangular shaped crystals.^{5,19,20} Less often observed hexagonal hBN crystals should have the sides with alternating nitrogen and boron terminations.

Here we show that the shape of synthesized hBN crystals drastically depends on the position of the copper foils in the furnace identified in Figure 1a. As shown in Figure 1b, the morphology of single domains deposited at 1065 °C slowly changes from triangular to truncate triangular and finally to pseudo hexagonal shape as the substrate position moves away from the CVD tube inlet. The changes occur because of misbalance between boron and nitrogen. The SEM images demonstrate that all shapes contain at least three straight edges which we attribute to those with nitrogen termination and are identified with blue color in the cartoon of Figure 1b. The truncated triangles, seen in the middle of the furnace, have three additional concaved edges, which, according to the hBN crystal structure, correspond to boron rich edges (red color in the cartoon). In pseudo hexagonal crystals, which grow closer to the tube outlet, boron rich edges become convex. Obviously,

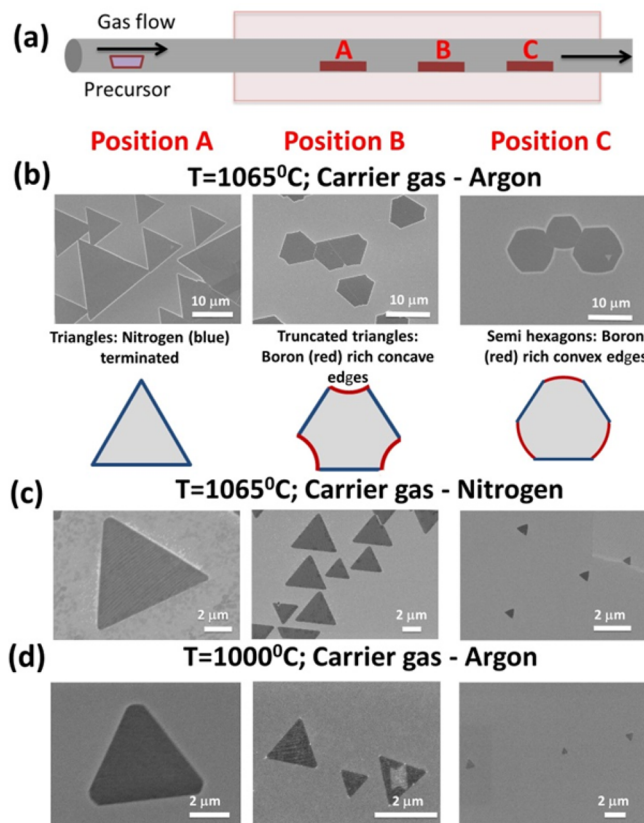


Figure 1. SEM images of the hBN crystals grown at different conditions. (a) APCVD experimental setup for hBN growth; ammonia borane precursor is in a separate nickel boat temperature for which $T_{ev} = 85$ °C was controlled either by position to the surface or by a separate heating. Copper substrates were placed at the positions A, B, and C with 8 in. distance between them. (b) SEM images of the hBN domains grown at 1065 °C using argon as a buffer gas. Sketch of the resulting hBN crystal shapes and corresponding termination—nitrogen (blue) and boron (red). (c) SEM images of the hBN domains grown at 1065 °C using nitrogen as a buffer gas and (d) growth at 1000 °C and using argon as a buffer gas.

the shape of these edges passes through a “straight cut”, that is, boron zigzag edges for foils' positions in between. We have not observed pure armchair edges such as hBN crystals in a form of nonagons.⁵ Such crystal shape evolution suggests different growth rates along the nitrogen and boron terminations. The nitrogen terminated edges remain unaffected and straight, suggesting a reduction in the available active nitrogen, at least on the surface of the copper catalyst, which causes the rate to drop in other directions. We associate the changes in the hBN crystal shape with deficiency of activated nitrogen containing species closer to the CVD tube outlet. The crystal growth rate can also define the crystal shape, but in our case it seems irrelevant as crystals of different shapes have similar sizes (Figure 1b) and crystals of similar shape have drastically different sizes (Figure 1c,d).

The thermal decomposition of ammonia borane ($\text{H}_3\text{N}-\text{BH}_3$) is quite complex (Figure 2).^{21–23} Major volatile products, which in our case are injected into the CVD tube inlet, include aminoborane ($\text{H}_2\text{N}=\text{BH}_2$), cyclic borazine ($\text{B}_3\text{N}_3\text{H}_6$), and molecular hydrogen (H_2). Minor amounts of diborane (B_2H_6) were also detected.²⁴ Solid byproducts are left in the precursor boat and include polyaminoborane ($([-\text{NH}_2-\text{BH}_2-]_n)$) which may be further transformed into the

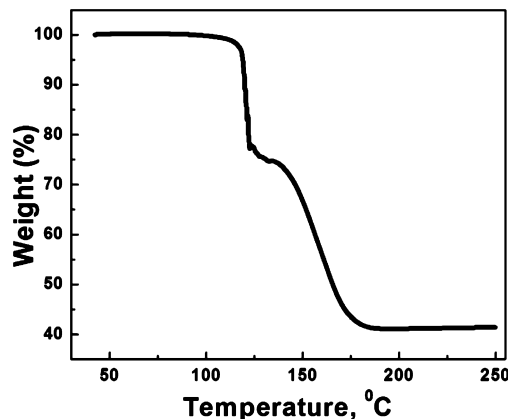


Figure 2. TGA curve for ammonia borane measured at the heating rate 5 °C/min in Ar carrier gas.

polyiminoborane ($(-\text{NH}=\text{BH}-)_n$) at higher temperatures ($T_{\text{ev}} > 130$ °C). The generated gaseous products of the ammonia borane decomposition can further polymerize and chemically transform inside the hot zone of the CVD tube. They do it more effectively on the surface of copper catalyst leading to dehydrogenation and production of hBN; we have not observed any deposition of hBN on quartz plates or SiO_2/Si wafers placed in the furnace at the same conditions.

Different disproportionation reactions that are responsible for misbalance between boron and nitrogen include diborane formation, high dissolution of boron in copper, and probably others.^{3,24–26} Both of these reactions must be accompanied by generation of nitrogen rich gases, which probably end up as inert molecular nitrogen given the high temperature of the synthesis and negative enthalpy of N_2 transformation to other compounds. Thus, the ratio of available activated boron and nitrogen species should increase along the tube and become higher than 1 (B:N > 1) closer to the tube outlet. Decrease in the available active nitrogen along the CVD tube length results in appearance of the boron reach edges, thus, gradually changing the crystal shape from triangular to pseudo hexagonal shape. Changing the buffer gas from argon to nitrogen leads to exclusively triangular shapes of hBN crystals throughout whole length of the CVD tube (Figure 1c). This drastic difference in the hBN crystal shape as compared to the growth in argon atmosphere can be explained by an additional source of active

nitrogen: boron activates readily available molecular nitrogen as a replenishing source of activated nitrogen species.²⁷ Intermediate species containing nitrogen further participate in hBN crystal growth resulting in nitrogen terminated triangular domain shape.

Similar effect can be achieved under argon by lowering the growth temperatures—deposition at 1000 °C with Ar buffer gas also results in exclusively triangular shaped crystals along the whole length of CVD tube (Figure 1d). We speculate that at a lower deposition temperature the equilibrium is not as drastically shifted toward formation of the molecular nitrogen as at higher temperatures; it keeps nitrogen in the activated form more effectively and leads to nitrogen terminated triangular crystals.

Hexagonal hBN crystal growth was reported previously, but the proposed mechanisms do not apply in our case. For example, Yin et al. attributed the presence of alternating N- and B-terminated zigzag edges in their low pressure CVD (LPCVD) to the enhanced concentration of Cu vapor inside the copper pockets.²⁸ Obviously, it cannot be applied in our case as APCVD synthesis precludes significant evaporation of the copper catalyst, thus raising doubt in the role of copper vapor. Tay et al. also observed the formation of hexagonal hBN and attributed it to the combined effect of surface oxygen on the Cu surface and enhanced lateral growth rate.²⁹ This mechanism cannot explain our observations either—we observe both triangular and hexagon shaped crystals on electropolished copper.

Domain Size and Orientation on the Copper Substrate. As Figure 3 illustrates, hBN growth at higher temperatures results in larger crystal sizes similar to what was observed for graphene synthesis in the past.¹⁷ Activation energy for hBN nucleation can be estimated from the Arrhenius plot as $E_{\text{nuc}} \sim 5$ eV, which is smaller compared to that of APCVD growth of graphene (9 eV).³⁰ Still, this E_{nuc} is high enough for a pronounced effect and results in 2 orders of magnitude decrease in the nucleation density by increasing the synthesis temperature by 100°, from 965 to 1065 °C (see Figure 3). DFT calculations suggest that adsorption energies of the B–N pair in hBN crystal on the Cu(111) surface is around 0.25 eV³¹ which is significantly higher compared to that of a pair of graphene carbon atoms on copper surface (0.06–0.13 eV).³² One can interpret that E_{nuc} may reflect a critical hBN nuclei size similarly to how it was done for graphene growth.³⁰ Taking the

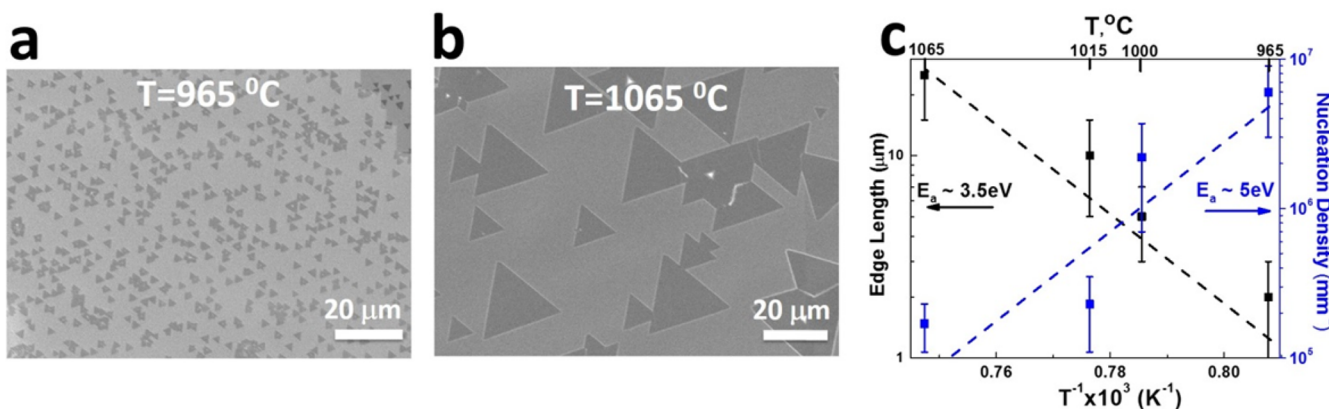


Figure 3. Effect of the growth temperature on the CVD grown hBN single domains. SEM image of hBN single domains at (a) 965 °C; (b) 1065 °C. (c) Arrhenius plot of the average edge length and the nucleation density versus growth temperature. The vertical error bars are standard deviations in statistical analysis. The samples were placed at the same position in the furnace (position A, see text), and deposition lasted 30 min.

adsorption energy for hBN on the copper surface from the DFT calculations, the measured $E_{\text{nuc}} \sim 5$ eV suggests that the critical nuclei size is ~ 20 BN pairs. It is significantly smaller than for graphene and implies that nucleation of hBN on copper can be achieved with much lower surface concentrations (supersaturations) of the precursors.

The size of hBN crystals increases significantly with increasing temperature showing an effective activation energy, $E_{\text{BN}} \sim 3.5$ eV (Figure 3). The largest crystals grown at 1065 °C reach 20 μm in size in 30 min, which further can be enlarged with time and by optimizing the precursor feeding rate. Because of the different activation energies of nucleation and growth, the rate of coverage also increases with temperature, thus suggesting that CVD at highest temperatures is most appropriate for hBN growth on Cu. Again, it is quite different from graphene, where that parameter was flat, making surface coverage nearly temperature independent in a broad range of temperatures.³⁰

Another distinction from graphene is the observation that hBN grows on copper epitaxially in a broad range of synthesis temperatures, 965–1065 °C. Copper foil used for hBN growth in this study has mixed crystallographic orientations,¹⁷ and we observe that most of the hBN crystals have parallel edges on individual copper domains (see, for example, Figure 1). Figure 4 provides a more rigorous analysis of the orientation of the edge for samples grown at different temperatures and various locations in the furnace.

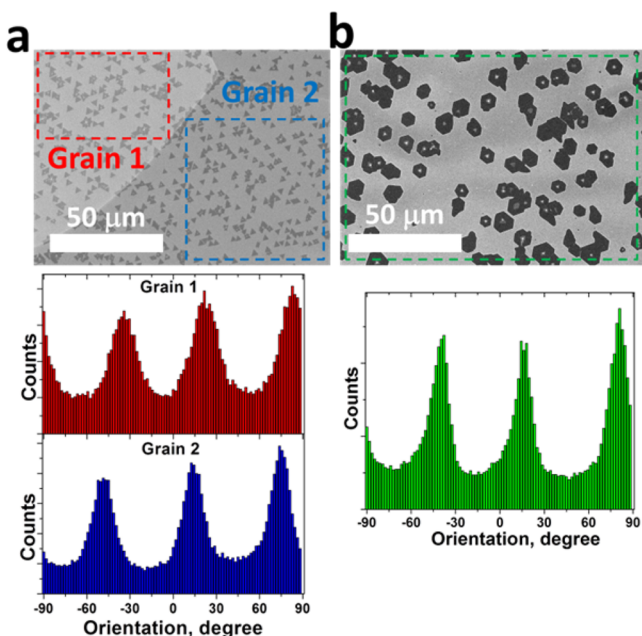


Figure 4. Analysis of the hBN crystals orientation on the copper foils suggests epitaxial growth on copper substrates. (a) SEM image of triangular crystals shows preferential hBN orientation on the different copper grains (red and blue). Histogram below SEM image shows orientation of triangle sides. A clear 60° pattern is seen. (b) same as (a), but for hexagonal hBN crystals.

Figure 4a shows the SEM image of the triangular crystals grown at 965 °C close to the inlet, while Figure 4b shows hexagonal hBN crystals grown at 1065 °C closer to the outlet. Note that the latter sample exhibits almost perfect hexagons with straight edges, rather than concave boron rich edges shown in Figure 1b, due to a slightly different position in the

furnace, where growth of boron and nitrogen edges had similar rates. Histograms below each SEM image in Figure 4 obtained similar to the previously described procedure^{33,34} illustrate that orientation of the crystals has a clearly recognizable 60° pattern. Different copper grains yield different preferred hBN orientations (Figure 4a) expected for epitaxy and ruling out other possible causes of hBN preferred orientation such as directed by the gas flow direction.

Growth of Complete hBN Monolayers. Similar to the graphene synthesis, increasing the growth time and/or precursor dosage leads to coalescence of hBN domains and eventually to formation of a complete hBN monolayer, sometimes with formation of 5,7 and 4,8 cycles grain boundaries.³⁵ Figure 5a shows an optical microscope image

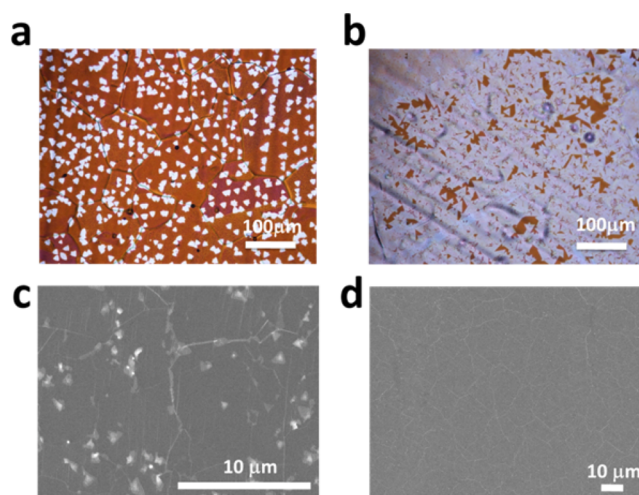


Figure 5. Synthesis of complete hBN films. (a) Optical image of oxidized copper surface with hBN triangular crystals (30 min growth at 1065 °C), (b) same as (a), but 45 min growth. Longer growth times result in hBN crystals coalescence with subsequent growth of complete film. (c) SEM image of complete film grown in 60 min using larger amount of precursor (7 mg). Bi- and trilayers are clearly seen. (d) same as (c), but precursor was slowly heated by the heating belt with the rate of 1 °C/min. Slow and controlled precursor heating resulted in hBN monolayer without apparent multilayers.

of a baked copper foil with triangular hBN domains grown for 30 min while 45 min growth results in a larger coverage presented in Figure 5b. Further increase in the growth time to 1 h produces complete hBN film (not shown herein). Alternatively, a complete film can be achieved in shorter growth time but using larger precursor mass. For example, Figure 5c shows that using 7 mg of precursor produces full coverage of copper foil by hBN film in 30 min while 3 mg of precursor are insufficient to achieve that, as demonstrated in Figures 5a,b. Faster growth rate compromises the quality of the hBN film—triangular hBN multilayers are clearly seen in the SEM image (Figure 5c). In addition to multilayers formation, larger precursor dosage probably results in smaller hBN domains and thus could potentially further diminish the quality of the resulting film. Controllable introduction of the precursor to the CVD chamber by gradual heating of the precursor using a heating belt wrapped around the precursor's location in the inlet of the CVD tube can lead to a much better quality of the film, similar to how it was employed in graphene growth. Moreover, a gradual raise in the precursor concentration allows elimination of the problems associated with nonuniform

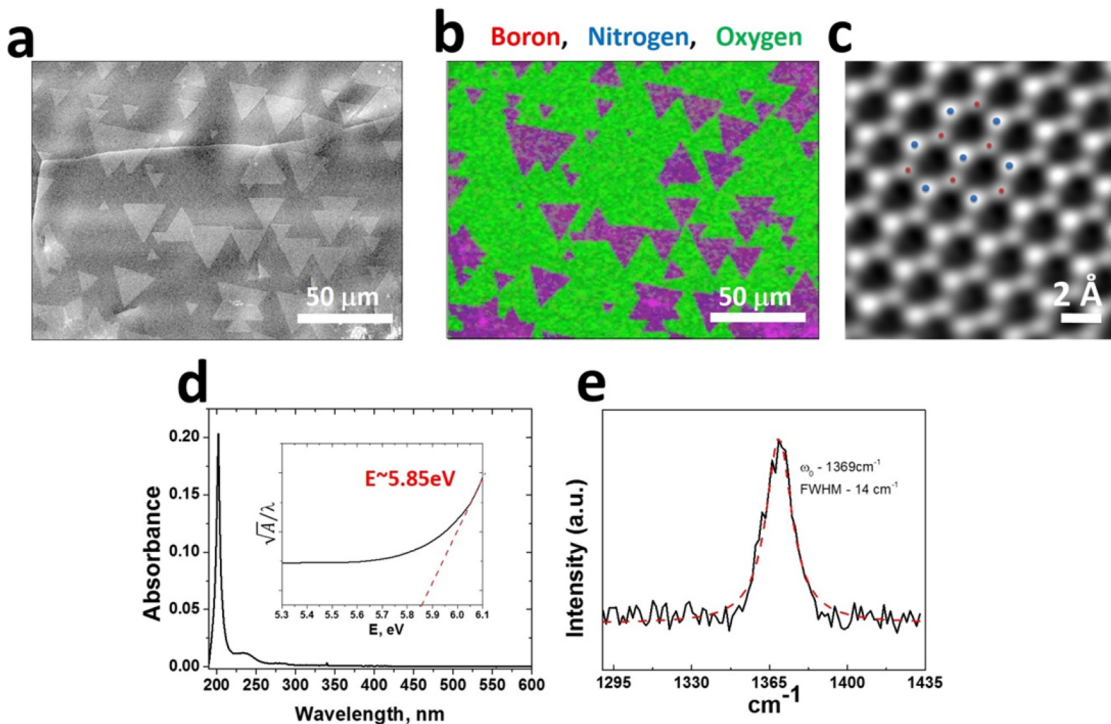


Figure 6. (a) SEM image and (b) the corresponding elemental map based on Auger spectra of hBN on Cu (boron as red, nitrogen as blue, and oxygen as green); oxygen appears from mild oxidation of Cu after synthesis. (c) Aberration-corrected STEM image of a single-layer hBN. The brighter atoms are nitrogen and lighter ones are boron; (d) UV/vis absorption spectrum of h-BN on quartz and the optical band gap analysis (inset) of monolayer hBN thin film; and (e) Raman spectrum of h-BN on SiO₂/Si substrate.

precursor distribution inside the CVD tube.¹⁷ For example, Figure 5d shows nearly perfect hBN monolayer grown using 7 mg of precursor (as Figure 5c), but aminoborane was gradually heated with 1 °C/min from $T_{ev} = 40$ to 100 °C. It resulted in lengthening the growth time compared to constant $T_{ev} = 85$ °C used in Figure 5c necessary for complete coverage. Thus, in order to get the best quality hBN monolayer films, the highest temperatures possible (below copper melting) should be used and precursor temperature should be gradually increased to temperatures not exceeding ~100 °C.

Characterization of hBN Monolayers. The monolayer films consist of relatively large single crystal domains of hBN and are of high quality without visible pinholes or ruptures as SEM images suggest (Figure 1b). The hBN crystals effectively prevent copper from oxidation as seen in Figure 5a. This is further supported by the Auger electron spectroscopy (AES) map in Figure 6a,b, where oxygen is green, nitrogen is blue, and boron is red. Atomic resolution annular dark-field STEM imaging shows the characteristic hexagonal hBN structure with the BN bond length of ~1.45 Å (Figure 5c). Based upon the atomic number dependence on image intensity,³⁶ line intensity profile measurements (Figure S3) were used to confirm that the brighter atoms are nitrogen as compared to boron.

The UV/vis absorption spectrum of the h-BN thin film transferred onto a quartz substrate is shown in Figure 6d and demonstrates almost zero absorbance in the visible range with significant absorbance only in the UV region. The optical band gap (OBG) estimated^{37,38} from the UV-vis spectrum of the h-BN is >5.85 eV, as shown in the inset in Figure 6d; it is close to the values reported elsewhere.¹⁶

Raman spectroscopy has proven to be a useful technique to analyze the characteristics of 2D materials including h-BN layers. The E_{2g} vibrational mode of hBN appears at 1366 cm⁻¹

for bulk boronitride and shifts to a higher frequency as the number of h-BN layers decreases. The Raman spectrum of our films exhibits a peak at 1369 cm⁻¹, which is consistent with previous reports for monolayer h-BN films.^{4,13} A highly symmetric Raman peak of narrow width indicates a high-purity h-BN single layer. Byproducts of borazine such as c-BN, B_xC_yN_z, and BN nanoparticles or polymer residue after the transfer process could all lead to Raman spectra alterations,² but apparently it is not significant in our case as the width is only 14 cm⁻¹.

CONCLUSIONS

We have elucidated the important parameters for atmospheric pressure CVD growth of hBN on copper such as the deposition temperature, thermal treatment of borazane precursor, and carrier gas composition. hBN crystals grow epitaxially on copper with large activation energy for both the nucleation ($E_{nuc} \sim 5$ eV) and growth ($E_{BN} \sim 3.5$ eV) processes suggesting that the highest temperatures are most suitable for growth of high quality hBN. At the same time, at high temperatures, hBN crystal shape change from triangular to truncated triangular and further to hexagonal depending on the substrate position in the furnace. hBN crystal shape evolution is explained by increasing the boron to nitrogen ratio along the CVD tube caused by generation of stable molecular nitrogen. The given explanation is supported by the growth at lower temperatures and synthesis under nitrogen atmosphere, both of which resulted in triangular hBN domains along the whole CVD tube length. Overexposure to the precursor (gaseous aminoborane decomposition products) leads to multilayer hBN films, while gradual increase in the precursor flow by controlled heating results in exclusively monolayer growth. To grow high quality hBN monolayer, the highest temperatures possible (below copper melting) should

be used, and precursor heating temperature should be gradually increased to temperatures not exceeding $\sim 100^{\circ}\text{C}$.

■ ASSOCIATED CONTENT

Supporting Information

The Supporting Information is available free of charge on the ACS Publications website at DOI: [10.1021/acs.chemmater.5b03607](https://doi.org/10.1021/acs.chemmater.5b03607).

SEM images with larger field of view shown in Figure 1b of main text; Auger electron spectroscopy maps of hexagonal hBN crystals; and atomic resolution imaging of single layer hBN ([PDF](#))

■ AUTHOR INFORMATION

Corresponding Authors

*E-mail: vlassioukiv@ornl.gov (I.V.V.).

*E-mail: snsn@nmsu.edu (S.N.S.).

Notes

The authors declare no competing financial interest.

■ ACKNOWLEDGMENTS

This research was supported by the Laboratory Directed Research and Development Program of ORNL, managed by UT-Battelle, LLC, for the U.S. Department of Energy. A portion of this research was conducted at the Center for Nanophase Materials Sciences, which is sponsored at Oak Ridge National Laboratory by the Scientific User Facilities Division, U.S. Department of Energy. The Oak Ridge National Laboratory is operated for the U.S. Department of Energy by UT-Battelle under Contract No. DE-AC05-00OR22725.

■ REFERENCES

- (1) Nagashima, A.; Tejima, N.; Gamou, Y.; Kawai, T.; Oshima, C. Electronic Structure of Monolayer Hexagonal Boron Nitride Physisorbed on Metal Surfaces. *Phys. Rev. Lett.* **1995**, *75*, 3918–3921.
- (2) Gorbachev, R. V.; Riaz, I.; Nair, R. R.; Jalil, R.; Britnell, L.; Belle, B. D.; Hill, E. W.; Novoselov, K. S.; Watanabe, K.; Taniguchi, T.; Geim, A. K.; Blake, P. Hunting for Monolayer Boron Nitride: Optical and Raman Signatures. *Small* **2011**, *7*, 465–468.
- (3) Lu, G.; Wu, T.; Yuan, Q.; Wang, H.; Wang, H.; Ding, F.; Xie, X.; Jiang, M. Synthesis of large single-crystal hexagonal boron nitride grains on Cu–Ni alloy. *Nat. Commun.* **2015**, *6*, 6160.
- (4) Ci, L.; Song, L.; Jin, C.; Jarirwala, D.; Wu, D.; Li, Y.; Srivastava, A.; Wang, Z. F.; Storr, K.; Balicas, L.; Liu, F.; Ajayan, P. M. Atomic layers of hybridized boron nitride and graphene domains. *Nat. Mater.* **2010**, *9*, 430–435.
- (5) Liu, Y.; Bhowmick, S.; Yakobson, B. I. BN White Graphene with “Colorful” Edges: The Energies and Morphology. *Nano Lett.* **2011**, *11*, 3113–3116.
- (6) Kim, K. K.; Hsu, A.; Jia, X.; Kim, S. M.; Shi, Y.; Hofmann, M.; Nezich, D.; Rodriguez-Nieva, J. F.; Dresselhaus, M.; Palacios, T.; Kong, J. Synthesis of Monolayer Hexagonal Boron Nitride on Cu Foil Using Chemical Vapor Deposition. *Nano Lett.* **2012**, *12*, 161–166.
- (7) Dean, C. R.; Young, A. F.; Meric, I.; Lee, C.; Wang, L.; Sorgenfrei, S.; Watanabe, K.; Taniguchi, T.; Kim, P.; Shepard, K. L.; Hone, J. Boron nitride substrates for high-quality graphene electronics. *Nat. Nanotechnol.* **2010**, *5*, 722–726.
- (8) Xue, J.; Sanchez-Yamagishi, J.; Bulmash, D.; Jacquod, P.; Deshpande, A.; Watanabe, K.; Taniguchi, T.; Jarillo-Herrero, P.; LeRoy, B. J. Scanning tunnelling microscopy and spectroscopy of ultra-flat graphene on hexagonal boron nitride. *Nat. Mater.* **2011**, *10*, 282–285.
- (9) Kim, K. K.; Hsu, A.; Jia, X.; Kim, S. M.; Shi, Y.; Dresselhaus, M.; Palacios, T.; Kong, J. Synthesis and Characterization of Hexagonal Boron Nitride Film as a Dielectric Layer for Graphene Devices. *ACS Nano* **2012**, *6*, 8583–8590.
- (10) Shi, G.; Hanlumyuang, Y.; Liu, Z.; Gong, Y.; Gao, W.; Li, B.; Kono, J.; Lou, J.; Vajtai, R.; Sharma, P.; Ajayan, P. M. Boron Nitride–Graphene Nanocapacitor and the Origins of Anomalous Size-Dependent Increase of Capacitance. *Nano Lett.* **2014**, *14*, 1739–1744.
- (11) Özçelik, V. O.; Ciraci, S. Nanoscale Dielectric Capacitors Composed of Graphene and Boron Nitride Layers: A First-Principles Study of High Capacitance at Nanoscale. *J. Phys. Chem. C* **2013**, *117*, 15327–15334.
- (12) Lim, H.; Yoon, S. I.; Kim, G.; Jang, A.; Shin, H. S. Stacking of Two-Dimensional Materials in Lateral and Vertical Directions. *Chem. Mater.* **2014**, *26*, 4891–4903.
- (13) Gao, Y.; Ren, W.; Ma, T.; Liu, Z.; Zhang, Y.; Liu, W.; Ma, L.; Ma, X.; Cheng, H. Repeated and Controlled Growth of Monolayer, Bilayer and Few-Layer Hexagonal Boron Nitride on Pt Foils. *ACS Nano* **2013**, *7*, 5199–5206.
- (14) Song, L.; Ci, L.; Lu, H.; Sorokin, P. B.; Jin, C.; Ni, J.; Kvashnin, A. G.; Kvashnin, D. G.; Lou, J.; Yakobson, B. I.; Ajayan, P. M. Large Scale Growth and Characterization of Atomic Hexagonal Boron Nitride Layers. *Nano Lett.* **2010**, *10*, 3209–3215.
- (15) Lee, K. H.; Shin, H.; Lee, J.; Lee, I.; Kim, G.; Choi, J.; Kim, S. Large-Scale Synthesis of High-Quality Hexagonal Boron Nitride Nanosheets for Large-Area Graphene Electronics. *Nano Lett.* **2012**, *12*, 714–718.
- (16) Shi, Y.; Hamsen, C.; Jia, X.; Kim, K. K.; Reina, A.; Hofmann, M.; Hsu, A. L.; Zhang, K.; Li, H.; Juang, Z.; Dresselhaus, M. S.; Li, L.; Kong, J. Synthesis of Few-Layer Hexagonal Boron Nitride Thin Film by Chemical Vapor Deposition. *Nano Lett.* **2010**, *10* (10), 4134–4139.
- (17) Vlassiuk, I.; Fulvio, P.; Meyer, H.; Lavrik, N.; Dai, S.; Datskos, P.; Smirnov, S. Large scale atmospheric pressure chemical vapor deposition of graphene. *Carbon* **2013**, *54*, 58–67.
- (18) Jacobberger, R. M.; Arnold, M. S. Graphene Growth Dynamics on Epitaxial Copper Thin Films. *Chem. Mater.* **2013**, *25*, 871–877.
- (19) Auwarter, W.; Suter, H. U.; Sachdev, H.; Greber, T. Synthesis of One Monolayer of Hexagonal Boron Nitride on Ni(111) From B-Trichloroborazine (ClBNH)₃. *Chem. Mater.* **2004**, *16*, 343–345.
- (20) Auwarter, W.; Muntwiler, M.; Osterwalder, J.; Greber, T. Defect Lines and Two-Domain Structure of Hexagonal Boron Nitride Films on Ni(111). *Surf. Sci.* **2003**, *545*, L735–L740.
- (21) Wolf, G.; Baumann, J.; Baitalow, F.; Hoffmann, F. P. Calorimetric process monitoring of thermal decomposition of B–N–H compounds. *Thermochim. Acta* **2000**, *343*, 19–25.
- (22) Kim, D.; Moon, K.; Kho, J.; Economy, J.; Gervais, C.; Babonneau, F. Synthesis and Characterization of Poly-(aminoborane) as a New Boron Nitride Precursor. *Polym. Adv. Technol.* **1999**, *10*, 702–712.
- (23) Frueh, S.; Kellett, R.; Mallory, C.; Molter, T.; Willis, W. S.; King'ondu, C.; Suib, S. L. Pyrolytic Decomposition of Ammonia Borane to Boron Nitride. *Inorg. Chem.* **2011**, *50*, 783–792.
- (24) Baitalow, F.; Baumann, J.; Wolf, G.; Jaenicke-Rößler, K.; Leitner, G. Thermal decomposition of B–N–H compounds investigated by using combined thermoanalytical methods. *Thermochim. Acta* **2002**, *391*, 159–168.
- (25) Lozovoi, A. Y.; Paxton, A. T. Boron in copper: A perfect misfit in the bulk and cohesion enhancer at a grain boundary. *Phys. Rev. B: Condens. Matter Mater. Phys.* **2008**, *77*, 165413.
- (26) Kidambi, P. R.; Blume, R.; Kling, J.; Wagner, J. B.; Baehtz, C.; Weatherup, R. S.; Schloegl, R.; Bayer, B. C.; Hofmann, S. In Situ Observations during Chemical Vapor Deposition of Hexagonal Boron Nitride on Polycrystalline Copper. *Chem. Mater.* **2014**, *26*, 6380.
- (27) Andrews, L.; Hassanzadeh, P.; Burkholder, T. R.; Martin, J. M. L. Reactions of pulsed laser produced boron and nitrogen atoms in a condensing argon stream. *J. Chem. Phys.* **1993**, *98*, 922.
- (28) Yin, J.; Yu, J.; Li, X.; Li, J.; Zhou, J.; Zhang, Z.; Guo, W. Large Single-Crystal Hexagonal Boron Nitride Monolayer Domains with Controlled Morphology and Straight Merging Boundaries. *Small* **2015**, *11*, 4497–4502.

- (29) Tay, R. Y.; Griep, M. H.; Mallick, G.; Tsang, S. H.; Singh, R. S.; Tumlin, T.; Teo, E. H. T.; Karna, S. P. Growth of Large Single-Crystalline Two-Dimensional Boron Nitride Hexagons on electro-polished copper. *Nano Lett.* **2014**, *14*, 839–846.
- (30) Vlassiuk, I.; Smirnov, S.; Regmi, M.; Surwade, S. P.; Srivastava, N.; Feenstra, R.; Eres, G.; Parish, C.; Lavrik, N.; Datskos, P.; Dai, S.; Fulvio, P. Graphene Nucleation Density on Copper: Fundamental Role of Background Pressure. *J. Phys. Chem. C* **2013**, *117*, 18919–18926.
- (31) Gómez Díaz, J. G.; Ding, D.; Koitz, D.; Seitsonen, A. P.; Iannuzzi, M.; Hutter, J. Hexagonal boron nitride on transition metal surfaces. *Theor. Chem. Acc.* **2013**, *132*, 1350.
- (32) Xu, Z.; Buehler, M. J. Interface Structure and Mechanics Between Graphene and Metal Substrates: a First-Principles Study. *J. Phys.: Condens. Matter* **2010**, *22*, 485301.
- (33) Liu, L.; Siegel, D. A.; Chen, W.; Liu, P.; Guo, J.; Duscher, G.; Zhao, C.; Wang, H.; Wang, W.; Bai, X.; McCarty, K. F.; Zhang, Z.; Gu, G. Unusual role of epilayer–substrate interactions in determining orientational relations in van der Waals epitaxy. *Proc. Natl. Acad. Sci. U. S. A.* **2014**, *111*, 16670–16675.
- (34) Wood, G. E.; Marsden, A. J.; Mudd, J. J.; Walker, M.; Asensio, M.; Avila, J.; Chen, K.; Bell, G. R.; Wilson, N. R. van der Waals epitaxy of monolayer hexagonal boron nitride on copper foil: growth, crystallography and electronic band structure. *2D Mater.* **2015**, *2*, 025003.
- (35) Li, Q.; Zou, X.; Liu, M.; Sun, J.; Gao, Y.; Qi, Y.; Zhou, X.; Yakobson, B. I.; Zhang, Y.; Liu, Z. Grain Boundary Structures and Electronic Properties of Hexagonal Boron Nitride on Cu(111). *Nano Lett.* **2015**, *15*, 5804–5810.
- (36) Krivanek, O. L.; Chisholm, M. F.; Nicolosi, V.; Pennycook, T. J.; Corbin, G. J.; Dellby, N.; Murfitt, M. F.; Own, C. S.; Szilagyi, Z. S.; Oxley, M. P.; Pantelides, S. T.; Pennycook, S. J. Atom-by-atom structural and chemical analysis by annular dark-field electron Microscopy. *Nature* **2010**, *464*, 571–574.
- (37) Yuzuriha, T. H.; Hess, D. W. Structural and optical properties of plasma-deposited boron nitride films. *Thin Solid Films* **1986**, *140*, 199–207.
- (38) Evans, D. A.; McGlynn, A. G.; Towlson, B. M.; Gunn, M.; Jones, D.; Jenkins, T. E.; Winter, R.; Poolton, N. R. J. Determination of the optical band-gap energy of cubic and hexagonal boron nitride using luminescence excitation spectroscopy. *J. Phys.: Condens. Matter* **2008**, *20*, 075233.